Journal of Glaciology, Vol. 34, No. 116, 1988

A STOCHASTIC MODEL OF ATMOSPHERIC RIME ICING

By E.M. GATES, A. LIU,

(Department of Mechanical Engineering, University of Alberta, Edmonton, Alberta T6G 2G8, Canada)

and E.P. LOZOWSKI

(Division of Meteorology, Department of Geography, University of Alberta,

Edmonton, Alberta T6G 2H4, Canada)

ABSTRACT. The accumulation of rime ice on structures, due to the impact and freezing of small water droplets, has been modelled as a stochastic process. Individual droplets are introduced into the flow field about the structure at a random position. Their trajectories are then calculated to determine the position of impact on the structure, or on previously impacted droplets. By assuming that the droplets maintain their shape on impact, the modelled accretion is gradually built up, one droplet at a time.

In the present paper, attention has been limited to a circular cylinder as the collecting structure, and it has been assumed that the flow field and the ice accumulation are strictly two-dimensional. With these assumptions, the influence of the droplet/cylinder diameter ratio and of the air speed upon the resulting predictions has been investigated. The main feature of interest in the model prediction is the development, near the edges of the accumulation, of discrete structures called "rime feathers". The mechanism for the growth of these rime feathers is described, and a comparison is made between the characteristics of the predicted structures and of some natural rime feathers grown in an icing wind tunnel.

INTRODUCTION

Atmospheric icing is the term used to describe the accumulation of ice on structures, due to the impact and freezing of cloud or fog droplets. Atmospheric rime icing, in particular, describes the icing process under conditions of air temperature, air speed, and water-mass concentration (liquid-water content), such that all the impinging water freezes on impact. Two distinguishing characteristics of rime ice accretions are: first, the development near the edges of the accretion of discrete elements called "rime feathers", such as those seen in the ice accretion on a wedge in Figure 1, or those described by Personne and others (1984); and secondly, a variation of ice density with position in the accretion. Current icing models like those of Ackley and Templeton (1979), Cansdale and Gent (1983), Lozowski and others (1983[a]), and Makkonen and Stallabrass (1984) cannot describe the growth of rime feathers, nor can they directly predict the density variation within the accretion. The difficulty is that, in each of these models, the effects of droplet impacts are averaged over intervals of time and area. In those parts of the accretion where the frequency of droplet impacts is high this averaging approach is appropriate. However, in regions near the edges of the accretion where the frequency of impacts is relatively low the averaging approach fails. In such regions, one might suspect that a stochastic modelling approach would be more suitable. Lozowski and others (1983[b]), for example, have demonstrated that a two-dimensional, Monte Carlo simulation can successfully predict some of the main features of rime-feather growth. As an alternative, then, to the approach taken in current models, we have chosen to model the accretion growth as a stochastic process, by extending Lozowski and others' idea to describe the growth of the *entire* accretion. In this paper we shall describe this technique and compare its predictions with some new experimental results.

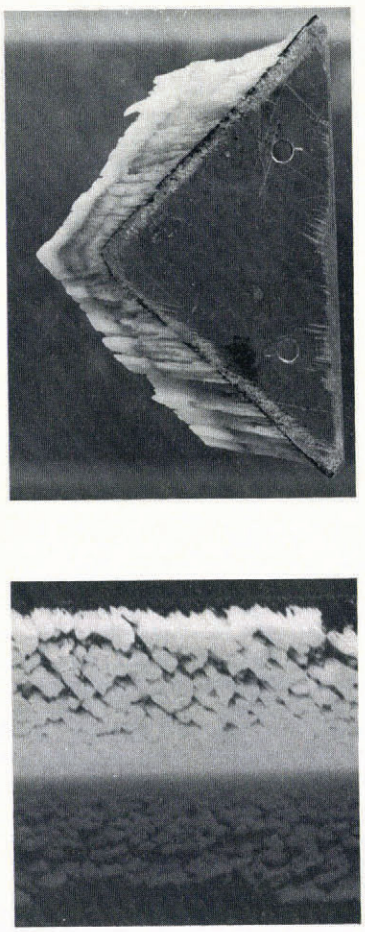

Fig. 1. Photographs of a 30 min rime-ice accretion on a 45° wedge. a. Silhouette of the accretion; b. Frontal view. Air speed: 11 m s^{-1}; air temperature: −9°C; liquid-water content: 1.1 g m^{-3}; droplet median-volume diameter: 20 μm.

DESCRIPTION OF THE MODEL

The physical situation to be modelled is summarized schematically in two-dimensional form in Figure 2, with a circular cylinder as the collector. The collector is exposed to a cold air stream laden with supercooled water droplets. As the air stream carries the droplets past the body, some of the droplets collide with the object, freeze, and adhere to

https://doi.org/10.3189/S0022143000009023 Published online by Cambridge University Press

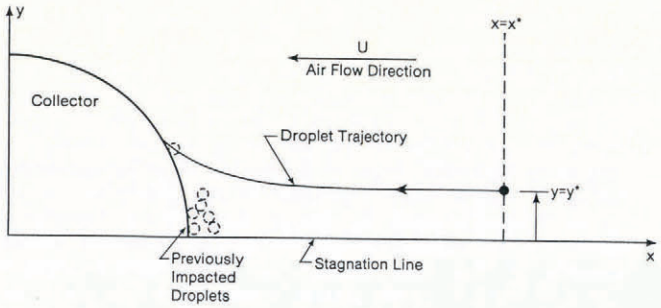

Fig. 2. A schematic drawing illustrating the physical situation that is modelled.

the surface. In existing models, the effects of the separate droplet impacts are integrated in area and time. The approach here, by contrast, is to consider each of the droplet impacts separately, and to construct the ice accretion one droplet at a time, assuming that the droplets freeze as spheres.

Although the method to be described is applicable to a fully three-dimensional case, attention here is limited to two dimensions. Thus, the ice collector, the flow field, and the structure formed by the freezing droplets are all assumed to be two-dimenaional. Attention has been limited to two dimensions initially, because of the great reduction in computational effort, and the ease with which the two-dimensional results can be presented and interpreted.

The approach is quite simple in concept, but rather difficult to put into practice, because of the large number of droplets that must be considered. It is a two-dimensional computational analogue of the ping-pong ball model constructed by Buser and Aufdermaur (1973). The procedure is first to choose randomly a droplet diameter from the known droplet-size distribution. Then, an initial starting ordinate (y^*) is also chosen randomly from a uniform spatial distribution. The initial abscissa (x^*) is fixed, however, and specified as ten body lengths up-stream. This coordinate is specified rather than chosen randomly, because it is necessary that the droplet be close to mechanical equilibrium with the air stream at its initial position. The droplet trajectory is now calculated in the potential flow around the target, using the equations of motion derived by Langmuir and Blodgett (1946), with the steady droplet-drag coefficients of Beard and Pruppacher (1969). The point of contact with the collector, or with a previously impacted droplet, can then be determined (see Fig. 2). Assuming that the droplet maintains a circular shape on impact and freezing, the accretion can be constructed, one droplet at a time. It is important to note that, in the present two-dimensional version of this model, the droplet centers are all assumed to lie in the plane of the simulation. Consequently, they are represented in the model by a circle of the same diameter as the droplet.

In the results presented here, we have restricted the general model described above by limiting the collector geometry to a circular cylinder. In addition, instead of dealing with a droplet-size spectrum, it has been assumed that the spray is mono-disperse. Finally, the extensive calculations associated with the determination of the droplet trajectory have been avoided by assuming a straight-line trajectory. Although the straight-line trajectory assumption is crude, it will be seen that the improvements made by including the trajectory curvature are not always worth the additional computational effort. A few of the simulations have, however, been made with the full trajectory calculations, and these will also be presented for comparison purposes.

With these simplifications, the only variables for the straight-line model are the ratio of the droplet diameter to the cylinder diameter, and the number of droplets introduced.

RIME-FEATHER GROWTH

The major features of the model predictions can be observed by considering the examples presented in Figure 3.

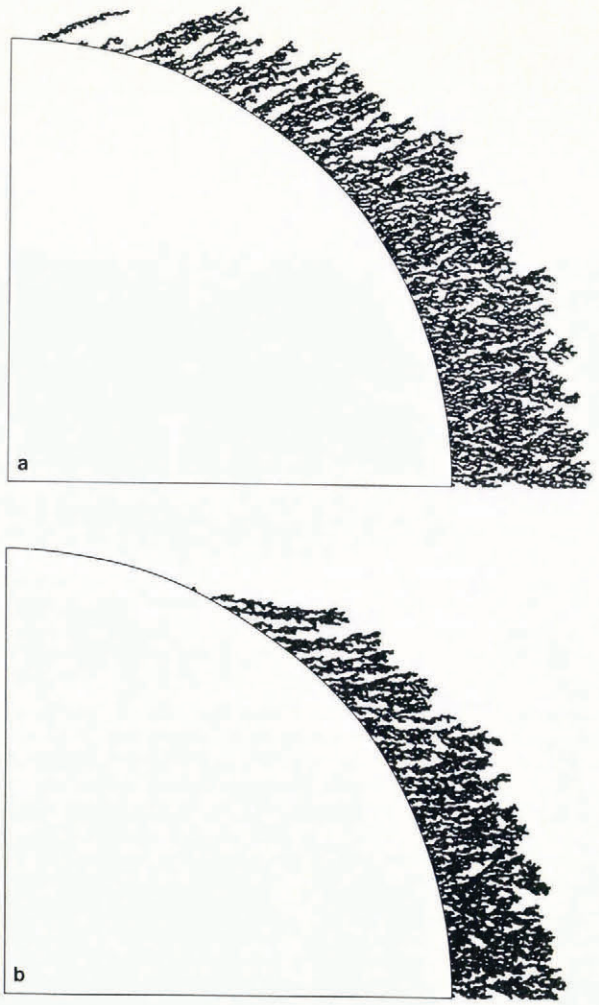

Fig. 3. a. An example of the straight-line model prediction for a cylinder/droplet diameter ratio of 508. Ten thousand droplets were introduced to produce this simulation.
b. An example of the full trajectory model prediction for a cylinder/diameter ratio of 508. An air speed of 5 m s^{-1} was used and 10 000 droplets were introduced to produce this simulation.

In order to produce these examples, 10 000 droplets were used with a cylinder/droplet diameter ratio of 508 : 1. This corresponds, for example, to 50 μm droplets collected by a 25.4 mm diameter cylinder. In Figure 3a, straight-line trajectories were used, whereas in Figure 3b the full trajectory calculations were carried out with an air speed of 5 m s^{-1}, and the other parameters as given above.

Even though the assumptions are rather limiting, the predictions are promising for several reasons. First, the simulations produce distinct structures at the edge of the accretion, bearing some resemblance to those produced by diffusion-limited aggregation (Sander, 1987). In the present case, however, these structures have a preferred growth direction. If the silhouette view in Figure 1 is compared with either of the predictions in Figure 3, it can be seen that in both the predicted and actual accretions the structures are separated by air gaps, start from a definite point on the surface, and grow in a generally up-stream direction. Although the two-dimensional predictions are not directly comparable with the full three-dimensional structures, these similarities suggest that the model does provide a reasonable description of the mechanism for rime-feather growth.

The mechanism for the formation of the rime feathers in the model simulations is "shadowing". As is illustrated in Figure 4, when a droplet hits the surface of the cylinder or a previously impacted droplet, the surface immediately down-stream is shaded from further collisions. This effect occurs over the entire surface but the shading is most pronounced where the angle, ψ, between the droplet trajectory at impact and the surface normal is large. This occurs at

https://doi.org/10.3189/S0022143000009023 Published online by Cambridge University Press

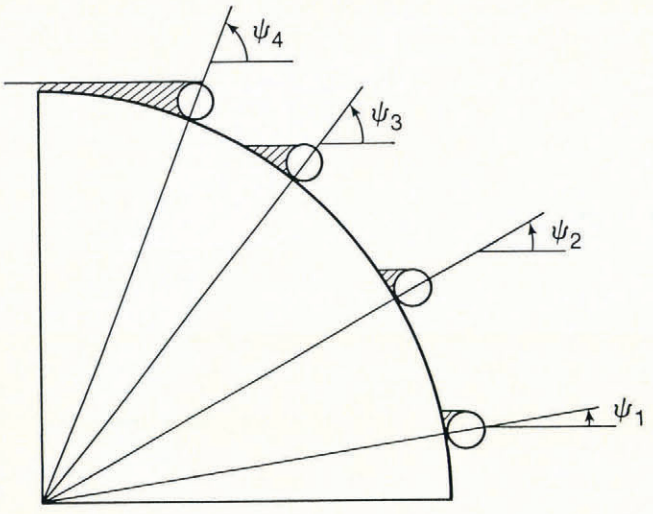

Fig. 4. A schematic drawing to illustrate the variation in the length of the shaded surface interval with position on the collector surface for straight-line trajectories.

the edges of accretion. The shadowing, at large angles, produces an open structure due to preferential growth of the stochastically favoured rime feathers. As can be seen in the simulations of Figure 3, several structures have started to grow at the edge of the accretion but shadowing by an up-stream structure, which has by chance grown faster, has prevented these structures from growing any further.

Moving from the edge of the accumulation towards the stagnation region, it can be seen from Figure 4 that the area shaded becomes smaller as the angle ψ decreases. A result of this reduction in shadowing is a closer packing than occurs at the edge of the accretion and the disappearance of discrete rime feathers. At the stagnation line itself, the angle between the surface normal and the trajectory is zero, and here shadowing is a minimum and there are no rime feathers.

Although the straight-line and curved-trajectory model predictions exhibit the same general features described above, there are some differences. These are best illustrated by examining again the predictions of Figure 3. The most obvious difference between the linear and curved-trajectory models is the extent of the accretion. In the straight-line prediction, accretion occurs over almost the entire up-stream surface of the cylinder, whereas in the prediction of the curved-trajectory model the lateral extent of the accretion is much less. A second difference is the predicted growth direction of the rime feathers. In the particular example shown in Figure 3, the growth angle relative to the free-stream direction is positive for the straight-line prediction but negative for the curved-trajectory prediction. In order to examine these two differences, and the predictions of the models in general, a series of simulations was carried out, with both the straight-line and curved-trajectory models. These were also compared with experimental simulations carried out in the University of Alberta FROST tunnel (Gates, 1981). The conditions and results of these simulations are summarized and presented in Tables I and II.

The differences in the extent of the accretion (as typified by the maximum impingement angle) and in the growth direction can be explained by examining the influence of droplet-trajectory curvature on the droplet–cylinder collisions and on rime-feather growth. Since the extent of the accumulations can be explained solely in terms of the effects of trajectory curvature, we will examine this factor first.

Figure 5a shows that, when the trajectories are straight lines, every point on the up-stream face of the cylinder is exposed to droplet collision at least initially. This situation will tend to occur in Nature when the drops are large, the cylinder small, and the air speed high. Normally, however, the droplets tend to be deflected away from the cylinder by the flow field. The magnitude of this deflection depends upon the droplet and cylinder diameters, and the air speed. As a consequence, there is some point on the surface beyond which no droplets will impact, as illustrated in Figure 5b. This position, as measured by the angle from the stagnation line, is called the maximum impingement angle (θ_{max}). For the nine simulations summarized in Table I, the predicted maximum impingement angle from the curved-

TABLE I. MAXIMUM IMPINGEMENT ANGLE. CYLINDER DIAMETER = 2.54 cm

Case number	*Air speed*	*Droplet diameter*	*Inertia parameter*	*Maximum impingement angle*		
				Straight line	*Curved*	*Experiment*
	m s^{-1}	μm				
1	10	18	0.9	90	45	62
2	10	27	1.9	90	60	60
3	10	37	3.6	90	69	64
4	20	17	1.6	90	55	64
5	20	30	4.8	90	72	72
6	20	36	6.9	90	75	72
7	30	18	2.5	90	63	60
8	30	27	5.9	90	73	68
9	30	32	8.3	90	77	75

TABLE II. RIME-FEATHER GROWTH DIRECTION

Case number	*Inertia parameter*	*Growth angle α*			*Growth angle α'*
		Straight line	*Curved*	*Experiment*	
1	0.9	16	−27	8	17
2	1.9	25	−5	8	25
3	3.6	23	−1	8	20
4	1.6	15	−20	−3	15
5	4.8	25	3	6	20
6	6.9	23	13	11	26
7	2.5	15	−10	−7	17
8	5.9	25	14	6	29
9	8.3	20	9	11	21

https://doi.org/10.3189/S0022143000009023 Published online by Cambridge University Press

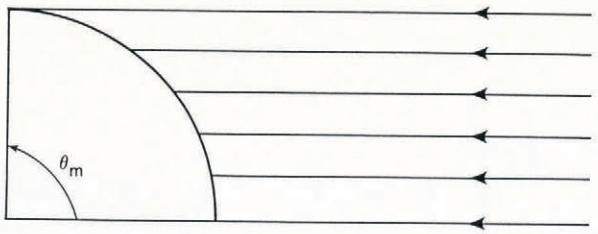

(a) straight-line trajectory

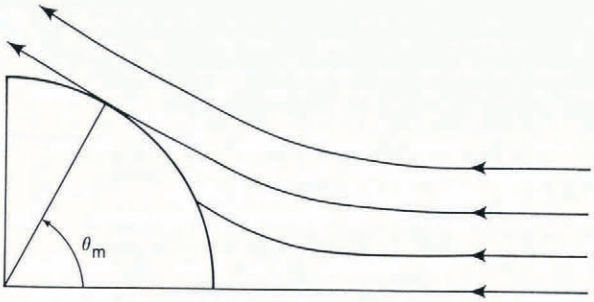

(b) curved trajectory

Fig. 5. The maximum impingement angle for the straight-line and curved-trajectory versions of the model.

trajectory model is presented in column 6. For all of these cases, the angle is substantially less than the 90° maximum impingement angle for the straight-line trajectory model.

The magnitude of the deflection of the droplet away from a straight trajectory is related to the inertia parameter, K (Langmuir and Blodgett, 1946). This parameter arises from the non-dimensionalization of the equations of motion for a droplet. It is defined as

$$K = \frac{\rho_d D_d U}{9\mu D_c}$$

where ρ_d is droplet mass density, D_d is droplet diameter, U is free-stream wind speed, μ is dynamic viscosity of air, and D_c is cylinder diameter.

A large value of the inertia parameter indicates that the droplet trajectory cannot easily be changed, and hence that the droplet will tend to follow a straight-line trajectory. The resulting collision efficiency will be close to unity. Similarly, if the inertia parameter is small, the droplet will tend to follow the flow stream lines about the cylinder and the collision efficiency will be reduced. In column 4 of Table I, the value of the inertia parameter for each of the nine cases is presented. The larger the value of the inertia parameter, the larger is the value of the maximum impingement angle. In the limiting case of a very large inertia parameter, the curved and straight-line versions of the model will predict the same maximum impingement angle.

The second difference between the straight-line and curved-trajectory model predictions is the growth direction of the rime feathers. To quantify this difference, an angle α is defined as that between the growth direction of a rime feather at the edge of the accretion and the free-stream wind direction. The model results for α are summarized in Table II. The straight-line trajectory model predicts that the growth direction, for the range of variables in the table, is always positive and varies between 15° and 25°. In the curved-trajectory model, the predicted growth angles are always less than those of the straight-line model, and in some cases α is negative. In order to explain these differences in the predicted rime-feather growth directions, it is necessary to examine how droplet-trajectory curvature influences the position of droplet—droplet impact.

Figure 6 illustrates the influence of increasing trajectory curvature on the impact position of an incoming

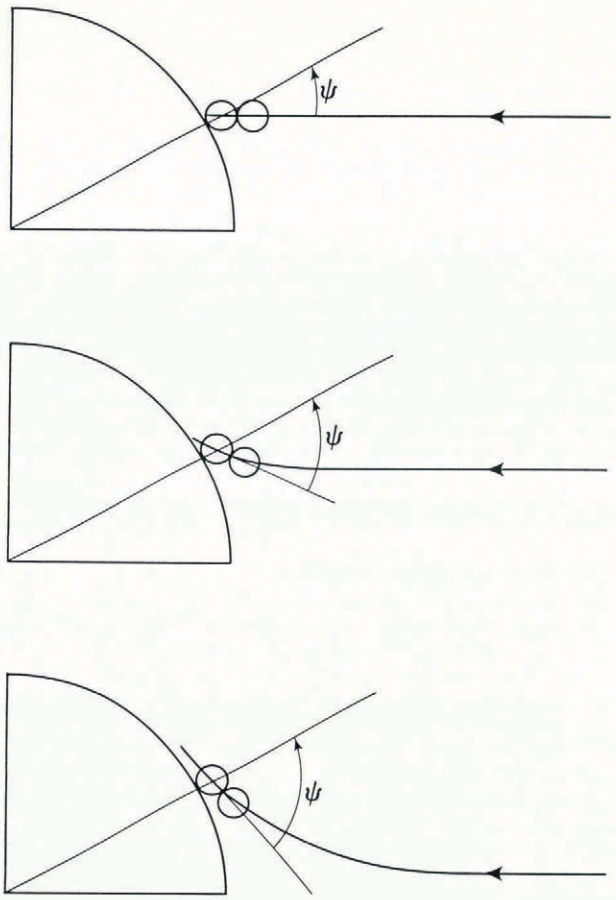

Fig. 6. The influence of droplet-trajectory curvature on the impact position of an incoming droplet whose trajectory passes through the centre of a previously impacted droplet.

droplet, whose trajectory passes through the centre of a previously impacted droplet. As the trajectory curvature is increased, the point of droplet—droplet contact is rotated clockwise. It could be expected, then, that the direction of growth of the rime feather would also be rotated in this direction. This suggests that, instead of comparing growth directions with the free-stream wind direction, they should be compared with the trajectory tangent at impact. In view of this idea, we define the angle α' to be that between the rime-feather growth direction and the trajectory tangent at impact. The α' values are summarized in column 6 of Table II. In terms of α', there is reasonable agreement between the growth directions for the curved and straight-line trajectory models (columns 3 and 6). This observation suggests that the rime-feather growth direction may be closely related to the angle between the droplet trajectory at impact and the surface normal, ψ.

For large values of K, the droplet trajectory approaches a straight line and the two model predictions differ by only a small amount, as illustrated in Table II and in Figure 6. For situations in which K is small, it is expected that the rime feathers will grow inward towards the stagnation line (a negative growth angle). As K increases, the growth angle will rotate towards positive values.

In the above discussion, we have examined how the two model predictions compare with each other but not whether the predictions are realistic. In order to obtain some information on the accuracy of the predictions, a series of nine experiments was carried out, in which rime-ice feathers were grown on a 2.54 cm diameter cylinder under the conditions summarized in Table I. The tests were not entirely successful, inasmuch as not all of the ice accretions were completely rime. Nonetheless, there were still recognizable preferred growth directions in the ice at

https://doi.org/10.3189/S0022143000009023 Published online by Cambridge University Press

the edge of each accretion. These were measured and are summarized in column 5 of Table II. The angles in this column are those between the growth direction and the wind direction, and should be compared with columns 3 and 4 in this table.

The measured values of the growth direction generally lie between the predictions of the straight-line and the curved-trajectory models. One might expect that the values should be closer to those of the curved-trajectory model, since the inertia parameters are small. However, this is not always the case. It is believed that the discrepancy is due to characterizing the droplet-size spectrum with a single-droplet size — the median-volume diameter. The magnitude of the median-volume diameter is influenced by all droplet diameters in the spectrum, whereas only the largest droplets in the spectrum are expected to contribute to the growth of the rime feathers. Using the median-volume diameter in the trajectory calculations results in higher droplet curvature, and hence a lower growth angle than using a diameter representative of the largest drops in the spectrum.

SUMMARY AND CONCLUSION

In this paper, we have described a stochastic model for the prediction of the accretion of ice on a structure due to freezing spray under dry icing conditions. In particular, attention has been focussed on the predictions of a two-dimensional model of ice accretion on a right-circular cylinder.

The stochastic model explains qualitatively the mechanism by which rime feathers are initiated and grow, i.e. down-stream shadowing coupled with competition among adjacent rime feathers. The version of the model employing the full trajectory calculations provides a more accurate estimate of the rime-feather growth direction than does the straight-line version. However, because the larger drops in an actual droplet spectrum are responsible for the growth of the feathers, use of the median-volume diameter to characterize the size spectrum is not appropriate. Probably, the best approach to pursue in future would be to incorporate the actual droplet spectrum into the model.

ACKNOWLEDGEMENT

The authors wish to acknowledge the support of this work by a contract with the Department of National Defence, through the Department of Supplies and Services, Canada, under contract agreement 2SU82-00334.

REFERENCES

Ackley, S.F., *and* Templeton, M.K. 1979. Computer modeling of atmospheric ice accretion. *CRREL Report* 79-4.

Beard, K.V., *and* Pruppacher, H.R. 1969. A determination of the terminal velocity and drag of small water droplets by means of a wind tunnel. *Journal of the Atmospheric Sciences*, **26**, 1066-72.

Buser, O., *and* Aufdermaur, A.N. 1973. The density of rime on cylinders. *Quarterly Journal of the Royal Meteorological Society*, **99**(420), 388-91.

Cansdale, J.T., *and* Gent, R.W. 1983. *Ice accretion on aerofoils in two-dimensional compressible flow. A theoretical model.* Farnborough, Royal Aeronautical Establishment. (Technical Report 82128.)

Gates, E.M. 1981. *FROST tunnel.* Edmonton, University of Alberta. Department of Mechanical Engineering. (Report 26.)

Langmuir, I., *and* Blodgett, K.B. 1946. A mathematical investigation of water droplet trajectories. *In* Langmuir, I. *Collected works. Vol. 10.* Oxford, Pergamon Press, 348-93.

Lozowski, E.P., Stallabrass, J.R., *and* Hearty, P.F. 1983[a]. The icing of an unheated, nonrotating cylinder. Part I: A simulation model. *Journal of Climate and Applied Meteorology*, **22**(12), 2053-62.

Lozowski, E.P., Stallabrass, J.R., *and* Hearty, P.F. 1983[b]. The icing of an unheated, nonrotating cylinder. Part II: Icing wind tunnel experiments. *Journal of Climate and Applied Meteorology*, **22**(12), 2063-74.

Makkonen, L.J., *and* Stallabrass, J.R. 1984. *Ice accretion on cylinders and wires.* Ottawa, National Research Council of Canada. (Technical Report TR-LT-005.)

Personne, P., Peigny, L., Soulage, M., *and* Soulage, R.G. 1984. Observation d'une forme particulière de givre sur des cables: quelle explication? *Journal de Recherches Atmosphériques*, **18**, 205-08.

Sander, L.M. 1987. Fractal growth. *Scientific American*, **256**, 94-100.

MS. received 25 March 1987 and in revised form 26 September 1987